Electronic Supplementary Material (ESI) for Energy & Environmental Science.

Carrier Trapping and Recombination: the Role of Defect Physics in Enhancing the Open Circuit Voltage of Metal Halide Perovskite Solar Cells

Tomas Leijtens[1,2], Giles E. Eperon[3], Alex J. Barker[1], Giulia Grancini[1], Wei Zhang[3],*

James M. Ball[1], Ajay Srimath Kandada[1], Henry J. Snaith[3], Annamaria Petrozza[1]*

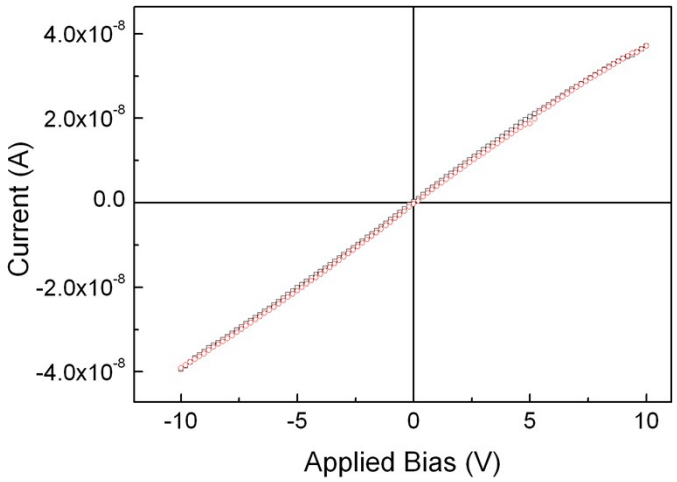

Figure S1. Current voltage curves of a flat perovskite sample laterally contacted by gold electrodes. The device is clearly functioning as a resistor. We have previously shown (by 4-point probe measurements) that the large spacing of electrodes (4 mm) means that the channel resistance is always much larger than the contact resistance[1]. Here, a potential was applied across two gold electrodes with 4 mm lateral spacing. Then the potential dropped between two small inner electrodes (corresponding to one third of the total channel length) was monitored on an autolabs potentiostat with 1Gohm input impedance. The potential dropped between these two electrodes was always one third of the total potential dropped between the two outer electrodes, indicating that contact resistance plays a negligible role in this measurement. As a result, the spacing between the electrodes makes no difference to the behavior we report in the main text, increasing the channel length would linearly reduce the measured photocurrent in the same way for all samples, leaving the trends unchanged.

Supplemental Discussion 1. The following discussion is to demonstrate that the photocurrent measured in the samples has no noticeable contribution from the PCBM or spiro quenching layers. Assuming a mobility of 10^{-3} cm^2 V^{-1} s^{-1} for electrons in PCBM[2,3], and considering the geometry of the sample (50 nm thick PCBM layer, 4 mm long and 4 mm wide channel), and the relation given in eq. 1 of the main text, we require an electron

density of 10^{20} cm^{-3} in the PCBM layer to match the photocurrent measured at the highest fluence, which corresponds to 1 sun's worth of light intensity. This is an absolutely unphysical charge density and would require electron lifetimes on the order of 50 ms in the fullerene even if every photoexcited electron in the perovskite were transferred. Since spiro-MeOTAD has an even lower hole mobility of around 10^{-4} cm^2 V^{-1} s^{-1}, it is even less likely to transport any significant amount of charge.
On the other hand, the photocurrents of 300 nA can be readily achieved with charge densities of 10^{16} cm^{-3}in a 300 nm perovskite layer even assuming just a mobility of 1 cm^2 V^{-1} s^{-1}.

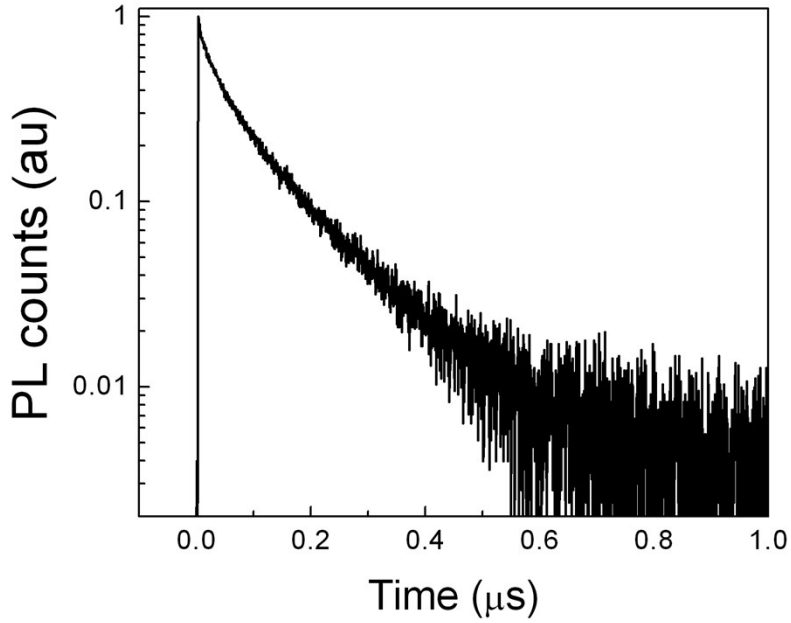

Figure S2. Photoluminescence decay at 10^{16} cm^{-3} excitation density, probed at 780 nm with 509 nm excitation wavelength.

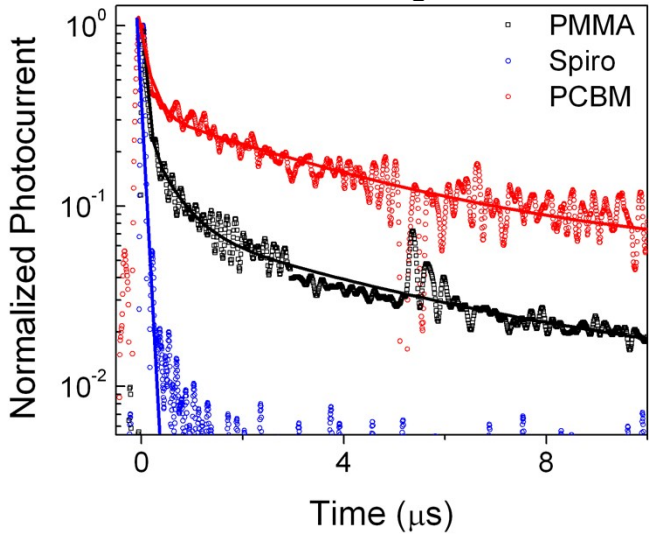

Figure S3. Photocurrent transients taken at 10^{15} cm^{-3} for PMMA, Spiro, and PCBM covered samples. The samples with PCBM on top show an initial quick decay on a time scale shorter than the instrument resolution, followed by an extremely slow decay over the course of tens of microseconds. The initial fast decay reduces the photocurrent signal

to approximately half its initial value. We interpret these results as follows: the first rapid decay corresponds to electron transfer from the perovskite to the PCBM with near unity efficiency as would be expected for this effective electron quencher[4,5], which leaves mobile holes in the perovskite which contribute to the photocurrent and only slowly recombine with the electrons in the PCBM. It appears that the recombination kinetics across the perovskite-PCBM interface are on the order of 10s of microseconds.

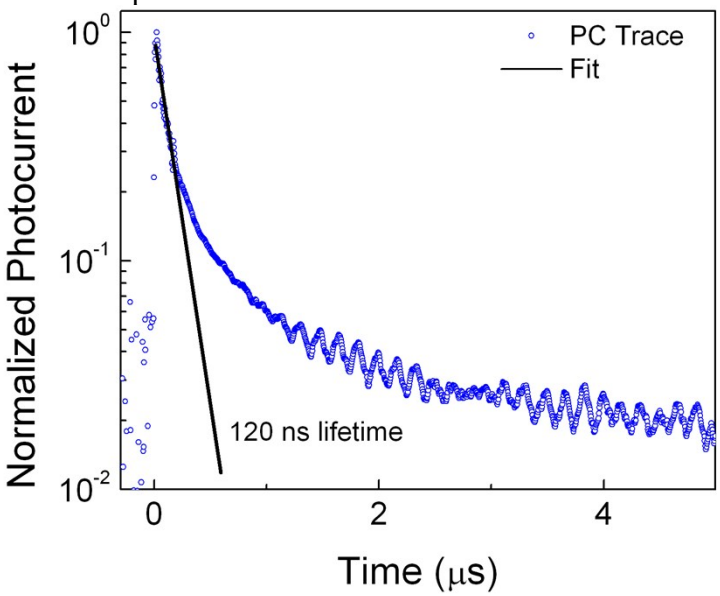

Figure S4. Normalized photocurrent trace of the PMMA covered sample taken at 10^{15} cm^{-3} excitation density. The first component of the trace is fit to a monoexponetial to demonstrate that the samples have a trapping lifetime of 120 ns, as has been previously reported for similar samples[4,6,7].

Discussion S2. With regard to the initial increase in sub gap photocurrent in the low background intensity regime, we can speculate that the materials also suffer from some hole traps which are more shallow and less high in density, which would fill up rapidly even with low excitation fluences. In addition, we have shown that the electronic trap distribution is extremely broad in energy (Figure 1b), and that the trap recombination kinetics do not follow simple monomolecular behavior (Figure 2). As a result, it is likely that trapped electrons will recombine with free holes differently depending on the depth of the trap site in question, with deeper traps (filled first) resulting in the most rapid recombination. This would also explain the initial rise in IR photocurrent: as some of the deeper traps are filled with weak above gap excitation, the effective recombination rate for modulated sub gap population (now in the higher energy traps) is lower and hence the steady state photocurrent is higher. In addition, it is possible that light irradiation may increase the trap density of perovskite materials by facilitating ion migration and this effect may initially be competing with trap filling in our initial measurements at low fluences.

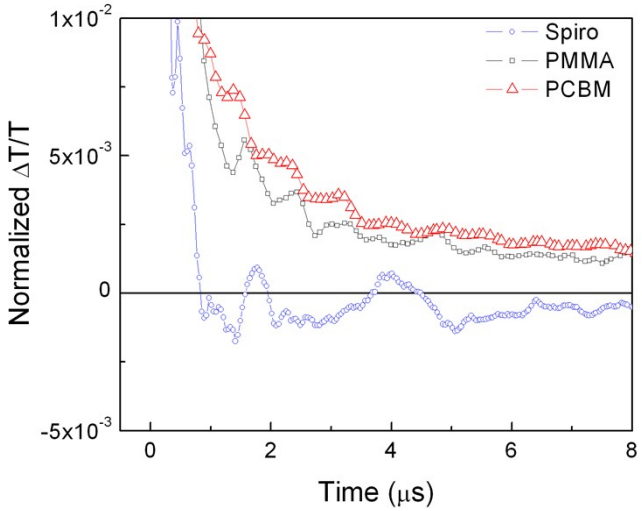

Figure S5. Zoomed in plot of the transient absorption plot (Figure 3 of main text) on a linear scale. This plot demonstrates that the Spiro contacted samples only display noise after 1 us after excitation, whereas the PMMA and PCBM contacted samples demonstrate a significant long lived tail.

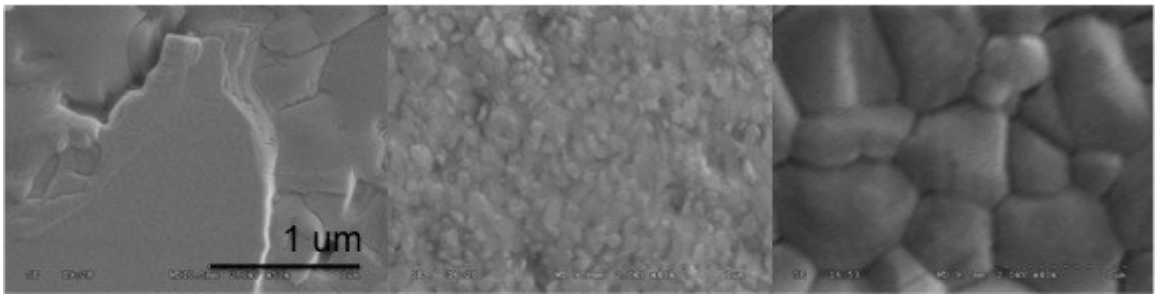

Figure S6. Scanning electron microscope images of $PbCl_2$, $PbAc_2$, and $PbAc_2$ + HPA derived perovskite films on glass.

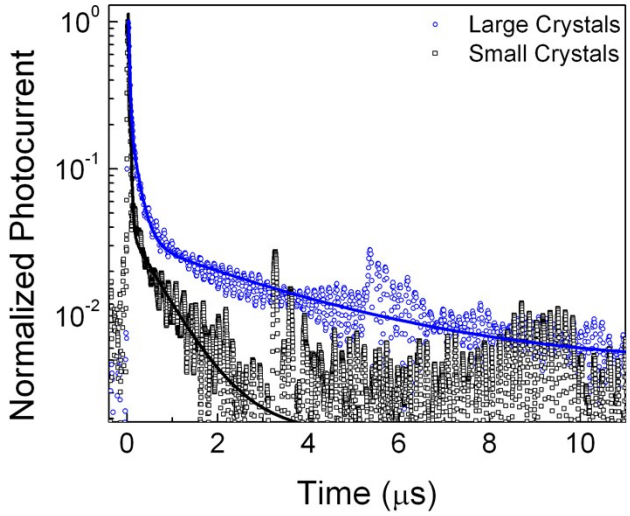

Figure S7. Transient photocurrent measurements as in Figure 2 of the main text for PMMA coated acetate derived perovskite films with (blue) and without (black) HPA treatment at 10^{16} cm^{-3} excitation density. The HPA clearly increases both the trapping lifetime as well as the timescale over which the trapped electrons recombine with the remnant free holes. The latter is an indication that films without HPA may even contain deeper trap sites through which recombination occurs more rapidly.

	G (cm^{-3} s^{-1})	n (cm^{-3})	p (cm^{-3})	Radiative Rate	PLQE (%)	Predicted V_{OC} 1 (V)	Predicted V_{OC} 2 (V)
100 ns trap recombination	2.9×10^{21}	2.9×10^{14}	2.9×10^{14}	7.4×10^{18}	0.3	1.143	1.147
Long Lived Holes	2.9×10^{21}	2.9×10^{14}	2.9×10^{16}	7.6×10^{20}	26	1.261	1.266

Discussion S2. It is possible to make some very simple estimations of what the fraction of radiative recombination will be for the two trap limited scenarios. Using the steady state electron and hole concentrations derived in Table 1 of the main text, we can simply calculate the radiative rate as R = n x p x B, where B is the bimolecular rate constant. We can then compare that rate to the total rate of recombination, which must be equal to the generation rate at open circuit, to determine the fraction of carriers that recombine radiatively (PLQE). We find that for the fast trap mediated recombination scenario, the PLQE at 1 sun's worth of excitation would be only 0.3 %, while it rises to approximately 26 % when accounting for the fact that the trapped electrons are actually long lived. In this latter case, it is clear that the numbers are rough approximations: we do not include the bimolecular recombination when evaluating the steady state carrier densities, but find that it is not completely insignificant. As a result, the estimated PLQE is likely to be a slight overestimate but certainly of the correct order of magnitude. The results show that it is essential to consider the fact that trapped electrons are long living to explain the high PLQEs (10-30%) reported in the literature. We can take this analysis one step further and use the estimated PLQEs to estimate the predicted V_{oc} for the solar cells using the simply relation $V_{OC} = V_{RAD} - KT\ln(PLQE)$, where KT is the thermal energy, and V_{RAD} is the radiative limit for the semiconductor, which is 1.3 for $MAPbI_3$. The V_{OC}s calculated this way are very similar to those calculated simply by considering the steady state carrier densities, lending credence to the values reported in Table 1 of the main text.

(1) Leijtens, T.; Stranks, S. D.; Eperon, G. E.; Lindblad, R.; Johansson, E. M. J.; McPherson, I. J.; Rensmo, H.; Ball, J. M.; Lee, M. M.; Snaith, H. J. Electronic Properties of Meso-Superstructured and Planar Organometal Halide Perovskite Films: Charge Trapping, Photodoping, and Carrier Mobility. *ACS Nano* **2014**, *8*, 7147–7155.

(2) Garcia-belmonte, G.; Munar, A.; Barea, E. M.; Bisquert, J.; Ugarte, I.; Pacios, R. Charge Carrier Mobility and Lifetime of Organic Bulk Heterojunctions Analyzed by Impedance Spectroscopy. **2008**, *9*, 847–851.

(3) Terao, Y.; Sasabe, H.; Adachi, C. Correlation of Hole Mobility, Exciton Diffusion Length, and Solar Cell Characteristics in Phthalocyanine/fullerene Organic Solar Cells. *Appl. Phys. Lett.* **2007**, *90*, 103515.

(4) Stranks, S. D.; Eperon, G. E.; Grancini, G.; Menelaou, C.; Alcocer, M. J. P.; Leijtens, T.; Herz, L. M.; Petrozza, A.; Snaith, H. J. Electron-Hole Diffusion Lengths Exceeding 1 Micrometer in an Organometal Trihalide Perovskite Absorber. *Science (80-.).* **2013**, *342* (6156), 341–344.

(5) Wojciechowski, K.; Leijtens, T.; Spirova, S.; Schlueter, C.; Hoerantner, M.; Wang, J. T.-W.; Li, C.-Z.; Jen, A. K.-Y.; Lee, T.-L.; Snaith, H. J. C60 as an Efficient and Stable N-Type Compact Layer in Perovskite Solar Cells. *J. Phys. Chem. Lett.* **2015**, *6* (12), 2399–2405.

(6) Zhang, W.; Saliba, M.; Moore, D. T.; Pathak, S. K.; Horantner, M. T.; Stergiopoulos, T.; Stranks, S. D.; Eperon, G. E.; Alexander-Webber, J. A.; Abate, A.; Sadhanala, A.; Yao, S.; Chen, Y.; Friend, R. H.; Estroff, L. A.; Wiesner, U.; Snaith, H. J. Ultrasmooth Organic-Inorganic Perovskite Thin-Film Formation and Crystallization for Efficient Planar Heterojunction Solar Cells. *Nat Commun* **2015**, *6*, 6142.

(7) Zhang, W.; Pathak, S.; Sakai, N.; Stergiopoulos, T.; Nayak, P. K.; Noel, N. K.; Haghighirad, A. A.; Burlakov, V. M.; deQuilettes, D. W.; Sadhanala, A.; Li, W.; Wang, L.; Ginger, D. S.; Friend, R. H.; Snaith, H. J. Enhanced Optoelectronic Quality of Perovskite Thin Films with Hypophosphorous Acid for Planar Heterojunction Solar Cells. *Nat Commun* **2015**, *6*.

(8) Deschler, F.; Price, M.; Pathak, S.; Klintberg, L. E.; Jarausch, D.-D.; Higler, R.; Hüttner, S.; Leijtens, T.; Stranks, S. D.; Snaith, H. J.; Atatüre, M.; Phillips, R. T.; Friend, R. H. High Photoluminescence Efficiency and Optically Pumped Lasing in Solution-Processed Mixed Halide Perovskite Semiconductors. *J. Phys. Chem. Lett.* **2014**, 1421–1426.

(9) Manser, J. S.; Kamat, P. V. Band Filling with Free Charge Carriers in Organometal Halide Perovskites. *Nat. Photonics* **2014**, *8* (9), 737–743.